



Published in final edited form as:

Nature. 2014 October 30; 514(7524): 642–645. doi:10.1038/nature13612.

Enhanced neonatal Fc receptor function improves protection against primate SHIV infection

Sung-Youl Ko¹, Amarendra Pegu¹, Rebecca S. Rudicell^{1,†}, Zhi-yong Yang^{1,†}, M. Gordon Joyce¹, Xuejun Chen¹, Keyun Wang¹, Saran Bao¹, Thomas D. Kraemer², Timo Rath², Ming Zeng^{3,†}, Stephen D. Schmidt¹, John-Paul Todd¹, Scott R. Penzak^{4,†}, Kevin O. Saunders¹, Martha C. Nason⁵, Ashley T. Haase³, Srinivas S. Rao¹, Richard S. Blumberg², John R. Mascola¹, and Gary J. Nabel^{1,†}

¹Vaccine Research Center, National Institute of Allergy and Infectious Diseases, National Institutes of Health, Building 40, Room 4502, MSC-3005, 40 Convent Drive, Bethesda, Maryland 20892-3005, USA

²Division of Gastroenterology, Department of Medicine, Brigham & Women's Hospital, Harvard Medical School, 75 Francis Street, Boston, Massachusetts 02115, USA

³Department of Microbiology, Medical School, University of Minnesota, 420 Delaware Street South East, Minneapolis, Minnesota 55455, USA

⁴Clinical Pharmacokinetics Laboratory, Pharmacy Department, Clinical Center, National Institutes of Health, Building 10, 10 Center Drive, Bethesda, Maryland 20814, USA

⁵Biostatistics Research Branch, Division of Clinical Research, National Institute of Allergy and Infectious Diseases, National Institutes of Health, 6700A Rockledge Drive, Room 5235, Bethesda, Maryland 20892, USA

Abstract

To protect against human immunodeficiency virus (HIV-1) infection, broadly neutralizing antibodies (bnAbs) must be active at the portals of viral entry in the gastrointestinal or cervicovaginal tracts. The localization and persistence of antibodies at these sites is influenced by the neonatal Fc receptor (FcRn)^{1,2}, whose role in protecting against infection *in vivo* has not been

©2014 Macmillan Publishers Limited. All rights reserved

Reprints and permissions information is available at www.nature.com/reprints.

Correspondence and requests for materials should be addressed to G.J.N. (Gary.Nabel@sanofi.com) or J.R.M. (jmascola@nih.gov).

[†]Present addresses: Sanofi, 640 Memorial Drive, Cambridge, Massachusetts 02139, USA (R.S.R., Z.-Y.Y. and G.J.N.); Center for Genetics of Host Defense, University of Texas Southwestern Medical Center, 5323 Harry Hines Boulevard, Dallas, Texas 75235-8505, USA (M.Z.); University of North Texas System College of Pharmacy, 3500 Camp Bowie Boulevard, RES-340J, Fort Worth, Texas 76107, USA (S.R.P.).

Author Contributions S.-Y.K., Z.-Y.Y., J.R.M. and G.J.N. designed the study, analysed the data and prepared the manuscript. A.P. analysed the data, set up the ADCC assay and provided the material for the ADCC assays. R.S.R. and K.O.S. helped to prepare the manuscript. M.G.J. performed the surface plasmon resonance analysis. X.C. performed DNA cloning and protein purification. T.D.K., T.R. and R.S.B. performed the transcytosis assay. S.B., M.Z. and A.T.H. performed immunohistochemical staining. S.D.S. and J.R.M. performed the neutralization assays. K.W., J.-P.T. and S.S.R. performed the pharmacokinetics and challenge study. S.R.P. analysed the pharmacokinetic data. M.C.N. conducted statistical analyses.

The authors declare no competing financial interests. Readers are welcome to comment on the online version of the paper.

Online Content Methods, along with any additional Extended Data display items and Source Data, are available in the online version of the paper; references unique to these sections appear only in the online paper.

defined. Here, we show that a bnAb with enhanced FcRn binding has increased gut mucosal tissue localization, which improves protection against lentiviral infection in non-human primates. A bnAb directed to the CD4-binding site of the HIV-1 envelope (Env) protein (denoted VRC01)³ was modified by site-directed mutagenesis to increase its binding affinity for FcRn. This enhanced FcRn-binding mutant bnAb, denoted VRC01-LS, displayed increased transcytosis across human FcRn-expressing cellular monolayers *in vitro* while retaining Fc γ RIIIa binding and function, including antibody-dependent cell-mediated cytotoxicity (ADCC) activity, at levels similar to VRC01 (the wild type). VRC01-LS had a threefold longer serum half-life than VRC01 in non-human primates and persisted in the rectal mucosa even when it was no longer detectable in the serum. Notably, VRC01-LS mediated protection superior to that afforded by VRC01 against intrarectal infection with simian–human immunodeficiency virus (SHIV). These findings suggest that modification of FcRn binding provides a mechanism not only to increase serum half-life but also to enhance mucosal localization that confers immune protection. Mutations that enhance FcRn function could therefore increase the potency and durability of passive immunization strategies to prevent HIV-1 infection.

Antibody protection against viral infection is influenced by effector functions mediated by the Fc domain of the antibody interacting with activating Fc receptors (including Fc γ RIIIa-mediated ADCC⁴) or inhibitory Fc receptors on the surface of immune cells⁵. FcRn is a multifunctional receptor that plays a role in IgG transport and homeostasis^{1,2}. FcRn binds to the Fc portion of IgG with high affinity at an acidic pH (<6.5). Following endocytosis, free IgG is degraded in the lysosome, while FcRn-bound IgG avoids degradation at low pH and is recycled into the extracellular space, thus prolonging the half-life of IgG^{1,2}. Recently, several monoclonal antibodies with broad and potent neutralizing activity against diverse HIV-1 Env proteins have been shown to confer passive protection against SHIV infection^{3,6–11,29}. To determine whether the protective efficacy of such antibodies can be increased by modulation of FcRn effector function, we evaluated the role of mutations that increase binding to FcRn. To potentiate the effector function of the bnAb VRC01, we introduced mutations in the CH2 and/or CH3 domains of VRC01 and analysed the binding affinity of these mutated antibodies for human FcRn and Fc γ RIIIa. Five mutants known to enhance binding to human FcRn (Fig. 1a), along with a non-FcRn-binding mutant (IHH)^{12–16}, were characterized *in vitro*. Similarly to VRC01, all mutants bound to a previously described HIV-1 Envprotein, RSC3 (which consists of a resurfaced, stabilized core³ of HIV-1 glycoprotein (gp) 120) (Fig. 1b); this finding is consistent with previously published reports of the effects of these FcRn-binding mutations on other IgGs¹⁴. All mutants also had similar neutralization potency and breadth to VRC01 (Extended Data Table 1). These data confirm that the FcRn-binding mutations did not interfere with the recognition of cognate antigen or with neutralization.

We also compared the ability of the FcRn-binding mutants to bind to human FcRn at physiological or endosomal pH (7.4 and 6.0, respectively). As expected, all mutants except VRC01-IHH bound more strongly to FcRn at either pH than did VRC01 (Fig. 1c). While the binding of the Fc mutants to human FcRn at pH 7.4 by enzyme-linked immunosorbent assay (ELISA) was greater than that of VRC01 at saturating antibody concentrations (>10 μ g ml⁻¹), differences in binding potency are best discriminated by using half-maximum binding

concentrations (EC_{50}). Analysis of EC_{50} values revealed greater binding by each of the FcRn-enabled mutants at pH 6.0 than at pH 7.4 (Extended Data Table 2), as expected and consistent with previous reports on the pH dependence of FcRn binding. It has been proposed that higher affinity binding to FcRn at pH 7.4 might inhibit the release of FcRn-bound IgG¹⁷. The FcRn-binding mutants of VRC01 were dissociated at pH 7.4 similar to VRC01 (Extended Data Fig. 1), indicating that VRC01 FcRn-binding mutations enhanced the pH-dependent binding but did not affect release at physiological pH.

FcRn affects the transport of IgG from the basolateral to the apical surface of mucosal epithelial cells¹. We therefore compared the transport of VRC01 and its FcRn-binding mutants across MDCK (Madin–Darby canine kidney) cells that express human FcRn and β_2 -microglobulin in a transwell system *in vitro*. When the concentration of monoclonal antibodies in the upper (apical) chamber was measured 2 h after antibody addition to the lower (basolateral) chamber, the transcytosis of all mutants with enhanced FcRn binding was at least 2.5-fold higher than that of VRC01. The highest level of transcytosis was exhibited by the VRC01-LS and VRC01-YTE mutants (Fig. 1d). These results show that mutations which enhance FcRn binding increase the transport of VRC01 in a functional cell culture system. To confirm this effect *in vivo*, we evaluated the pharmacokinetics of these antibody mutants in human FcRn-transgenic mice¹⁸ ($n = 4$ per group). Similar to the cell culture results, all mutants with enhanced binding to human FcRn had a longer half-life than VRC01 (Extended Data Fig. 2).

In addition to virus neutralization, another Fc effector function has been implicated in immune protection. ADCC, which is mediated by IgG binding to Fc γ RIIIa, can lyse infected cells^{4,19}. Because enhanced FcRn-binding mutations might affect the interactions of IgG with Fc γ RIIIa and thereby alter ADCC activity¹³, we assessed the Fc γ RIIIa binding and ADCC effector function of each mutant. We performed ELISA binding assays with human Fc γ RIIIa and ADCC assays using human peripheral blood mononuclear cells as effector cells and HIV-infected CEM-NK^R cells (a natural killer (NK)-cell-resistant human T leukaemia cell line) as targets²⁰. Most of the enhanced FcRn-binding mutants showed lower Fc γ RIIIa binding and ADCC activity than VRC01. Interestingly, only the VRC01-LS mutant exhibited both Fc γ RIIIa binding and ADCC activity comparable to VRC01 (Fig. 1e, f). We further examined the binding affinities of VRC01-LS for human FcRn and Fc γ RIIIa using surface plasmon resonance analysis. Consistent with the ELISA results, VRC01-LS exhibited a 12-fold higher human FcRn binding affinity than VRC01, whereas both displayed similar binding to human Fc γ RIIIa (Table 1). These data suggested that the increased FcRn binding of VRC01-LS did not affect its Fc γ RIIIa-mediated effector function. We further examined the binding of these VRC01 variants to two other functional IgG receptors, Fc γ RIIa and Fc γ RIIb. We found no difference in the binding of VRC01 and VRC01-LS to either receptor, as determined by ELISA (Extended Data Fig. 3), suggesting that VRC01-LS does not differ from VRC01 with respect to ADCC effector function or immune suppression through Fc γ RIIa or Fc γ RIIb, respectively.

Because its ADCC activity was not affected by the FcRn-binding mutation, we selected the VRC01-LS mutant for further analysis in nonhuman primates. Its half-life *in vivo* was evaluated by injection (10 mg per kg body weight) and compared with VRC01, and VRC01-

IHH, in Indian rhesus macaques (*Macaca mulatta*). The serum concentrations of each monoclonal antibody were measured by ELISA, and the half-lives were calculated using a two-compartment model (Fig. 2a). The LS mutant had a 2.5-fold longer half-life (VRC01, 4.65 days; VRC01-LS, 11.80 days) and a 2.5-fold slower clearance rate than the wild type (VRC01, 16.52 ml day⁻¹ kg⁻¹; VRC01-LS, 6.47 ml day⁻¹ kg⁻¹). By contrast, VRC01-IHH displayed markedly less persistence than the wild type, with a half-life of <1 day. This result confirmed that the increase in FcRn binding of VRC01-LS prolonged the antibody's half-life in non-human primates.

Since the gut mucosa is a primary site of HIV infection, we examined the accumulation of each monoclonal antibody in the rectal mucosa. Because direct tissue immunohistochemical staining is subject to sampling variation, we used a more quantitative approach: we quantified the total amount of VRC01 or VRC01-LS in rectal tissue homogenates, by using ELISA. Protein was extracted from rectal biopsy samples, and the amount of each monoclonal antibody was normalized to the total amount of tissue protein. After a single injection (10 mg kg⁻¹), VRC01-LS remained detectable in rectal tissue for more than 70 days and persisted at significantly higher levels than VRC01 ($P < 0.001$, two-tailed t -test), which was not detected after 28 days (Fig. 2b). VRC01-IHH was not detected in rectal tissues after 14 days. At lower concentrations of monoclonal antibody (0.3 mg kg⁻¹), a similar trend was seen in both the serum and the rectal mucosa. The levels of VRC01 in rectal tissue peaked at day 2, whereas VRC01-LS continued to increase up to day 5, after which it persisted at higher levels than VRC01 (Fig. 3a). In parallel studies, we also compared the relative monoclonal antibody levels in rectal secretions and tissue in cynomolgus macaques (*Macaca fascicularis*). Similarly to rhesus macaques, VRC01-LS circulated for threefold longer in the serum than did VRC01 (Extended Data Fig. 4a). Compared with VRC01, higher levels of VRC01-LS were measured in both rectal secretions and tissue at 28 days post antibody infusion, although the rectal tissue sampling was more consistent than the secretions (Extended Data Fig. 4b, c). We therefore suggest that tissue IgG provides an important indicator of mucosal IgG localization, consistent with a previous report²¹.

To determine whether VRC01 co-localized with FcRn *in vivo*, rectal biopsy samples taken after a single injection were stained either with a polyclonal antibody specific for human FcRn or with an HIV-1 Env probe, RSC3 (ref. 3). FcRn co-localized with VRC01 mainly in mucosal epithelial cells (Fig. 2c). Together, these data demonstrated that VRC01-LS persisted longer in the serum than VRC01 and accumulated in the mucosa as a result of its increased binding affinity for FcRn.

To determine whether VRC01-LS can protect against infection more effectively than VRC01, we performed an intrarectal challenge with the CC-chemokine receptor 5 (CCR5)-tropic SHIV BaLP4. Rhesus macaques ($n = 12$ per group) were injected intravenously with a low, suboptimally protective, dose (0.3 mg kg⁻¹) of VRC01, VRC01-LS or control IgG and challenged intrarectally with SHIV 5 days after passive antibody transfer. All control-IgG-injected macaques became infected within 3 weeks of SHIV challenge, as measured by plasma viraemia. Ten of 12 macaques that received VRC01 were infected, in contrast to 5 of 12 VRC01-LS-injected macaques ($P = 0.0447$, one-tailed Fisher's exact test) (Fig. 3b and

Extended Data Fig. 5). Among the infected animals, no significant differences in peak or set-point viraemia were observed between these experimental groups. VRC01-LS therefore conferred superior protection to VRC01 against acquisition of lentiviral infection.

In this study, we show that modification of a monoclonal antibody–FcRn interaction through mutations in the Fc domain can increase the protection afforded by the antibody against mucosal lentiviral challenge. Passive infusion of anti-HIV-1 bnAbs has been shown to prevent mucosal SHIV infection²², and the pharmacokinetics and biodistribution of the bnAbs play important roles in this protection²¹; however, the mechanism that confers mucosal protection has not been defined. Specifically, whether antibody transport and FcRn effector function contribute to mucosal immunity in primates was previously unknown. Our work demonstrates that FcRn plays an important role in IgG transport and provides insight into the mechanism by which FcRn function facilitates protection by IgG against mucosal viral infection. The increased FcRn binding of IgG induced by the LS mutation avoids endosomal degradation, allowing recycling into the serum, thereby increasing the serum antibody levels. The antibody retention in the rectal mucosa is probably due to antibody sequestration in the endosomes of epithelial cells (as indicated by the intracellular localization, Fig. 2c), which is presumably followed either by recycling into the subepithelial mucosal tissue for interactions with professional antigen presenting cells or by transcytosis into the intestinal lumen. Importantly, this mutation also increased the retention of IgG in the intestinal mucosa at the portal of HIV-1 entry, where a higher local concentration can more effectively neutralize local infection.

Our results suggest that active, FcRn-mediated transport, as opposed to simple diffusion, is a major component of IgG compartmentalization in the mucosal tissues of the rectum. FcRn-mediated transport of IgG to mucosal surfaces may play an unrecognized role in the ability of a variety of vaccines to successfully block mucosal viral infections. For example, vaccination with inactive poliovirus (also known as the Salk vaccine) generates an IgG response that can block poliovirus infection in the gut mucosa²³. There are similarities, as well as potential differences, between poliovirus and HIV-1 pathogenesis. Both poliovirus and HIV-1 invade the human body through mucosal tissues, especially the intestinal mucosa, but the receptors for cell entry are different. Poliovirus penetrates the body through M cells, in the Peyer's patches²⁴, whereas HIV-1 targets intraepithelial CD4⁺ T cells in the mucosal epithelium. Although FcRn mediates the transcytosis of IgG across the intestinal epithelium *in vivo* as has been shown in a humanized mouse model²⁵, our results demonstrate that FcRn is also a means to retain IgG in tissues. This latter effect may restrain the quantities of IgG that are transported into the lumen and potentially explains why previous studies have failed to find an association between monoclonal antibody levels in mucosal secretions and protection²¹. Macaques with higher levels of bnAbs (VRC01-LS) in rectal tissues had a lower rate of infection than macaques injected with VRC01 (Fig. 3). Thus, it is important to measure IgG in tissues, in addition to in mucosal secretions.

The sexual transmission of HIV-1 is initiated by the replication of one or a small number of virions that penetrate the vaginal or rectal mucosa²⁶. The FcRn-mediated anatomical localization of bnAbs to the rectal mucosa may more effectively block penetration at this site of entry. This localization, combined with the quantitative effects of FcRn on serum IgG

levels, explains how increasing the affinity for FcRn improves bnAb efficacy. Notably, FcRn expression has also been reported in the female genital tract²⁷: FcRn knockout in this previous paper was associated with decreased IgG-mediated protection against intravaginal herpes simplex virus (HSV-2) challenge. Because the FcRn knockout effects are global, it is unclear whether this effect was mediated through a systemic or mucosal effect; nonetheless, together, these studies are complementary and support the idea that FcRn mediates mucosal protection by IgG. The potential role of FcRn at other mucosal sites is further supported by the observation that VRC01 accumulates in vaginal tissues and localizes to the basal and parabasal layers of the vaginal epithelium, similarly to FcRn, as determined by immunohistochemistry (Extended Data Fig. 6). Presumably, FcRn-mediated transport increases the monoclonal antibody levels in this tissue, where it might similarly confer protection against infection.

Altering the pharmacokinetic profile of antibodies by increasing half-life and tissue localization has practical implications for the use of passive monoclonal antibody administration for immunoprophylaxis and therapy. One concern about the use of such monoclonal antibody mutations is whether they might elicit immune responses to the FcRn-binding mutation. We found no evidence of increased antibody responses to VRC01-LS or specifically to the LS mutation relative to VRC01 (Extended Data Fig. 7). Because VRC01 is human and xenogeneic to non-human primates, such questions about immunogenicity must eventually be evaluated in humans. In this regard, at least one human monoclonal antibody with an FcRn-binding-site mutation (motavizumab-YTE; M252Y / S254T / T256E) has been tested in healthy human adults and did not induce an appreciable increase in an anti-drug antibody response compared with the wild-type antibody²⁸.

Potent bnAbs with increased FcRn binding can be retained in relevant tissues for extended periods, decreasing the necessary amount of antibody, as well as the frequency of injections, thereby making the treatment or prevention of viral infections by passive antibody transfer more feasible than at present and broadly applicable. In addition to its potential importance for the optimization of passive immune prevention of HIV-1 infection of humans, this mechanism is also likely to be relevant to antibody-mediated protection against other mucosal pathogens such as rotavirus, poliovirus, norovirus and influenza virus.

METHODS

Generation and characterization of VRC01 Fc mutants

The Fc mutations used in this study are indicated in Fig 1a. The amino acid positions are numbered according to the EU index of human IgG1 (ref. 30). Mutations were introduced to the heavy chain gene of VRC01 by site-directed mutagenesis using the QuikChange II Site-Directed Mutagenesis Kit (Agilent Technologies). Mammalian expression plasmids encoding the heavy and light chain genes were transiently co-transfected into the human embryonic kidney cell line 293F, and the supernatant was harvested 5 days later. The monoclonal antibodies were purified from the supernatant by Protein G column chromatography (GE Healthcare).

The glycosylation patterns of VRC01 and VRC01-LS were analysed by using nanoLC-ESI-MS/MS (nano liquid chromatography electrospray ionization mass spectrometry) peptide sequencing technology. In brief, each solution sample was cleaned and digested in-gel with sequencing grade modified trypsin (Promega). The resultant peptide mixture was analysed by an LC-ESI-MS/MS system, in which high performance liquid chromatography (HPLC) with a 75- μm (inner diameter) reverse phase C18 column was coupled in-line with an ion trap mass spectrometer (Thermo Scientific). Comparing the glycosylation patterns of VRC01 and VRC01-LS by mass spectrometry, we focused on the glycan at amino acid position N297, which is the single *N*-glycosylation site in the Fc region of IgG1 isotype antibodies (such as VRC01). A very similar pattern of complex glycan configuration was noted for both monoclonal antibodies (Extended Data Table 3). G1F (GalGlcNAc₂Man₃GlcNAc₂Fuc) and G0F (GlcNAc₂Man₃GlcNAcFuc) are the major glycosylation species found in both VRC01 and VRC01-LS. While quantitative differences were noted in some glycan species, these differences represent small changes and fall within the limits of the expected experimental variability between preparations. More importantly, the LS mutation neither generated nor removed additional potential *N*-linked glycosylation patterns observed in VRC01.

ELISA

RSC3 ELISAs were used to analyse IgG binding. ELISA plates (96 well) were coated with 2 $\mu\text{g ml}^{-1}$ RSC3 in PBS, incubated at 4 °C overnight and blocked with PBS containing 5% BSA at room temperature for 1 h. Serial dilutions of each monoclonal antibody in 2.5% BSA in PBS were added to the plates and incubated at room temperature for 1 h. Horseradish peroxidase (HRP)-conjugated anti-human IgG, Fc γ -specific (Jackson ImmunoResearch Laboratories), was added and incubated at room temperature for 1 h. Tetramethylbenzidine (TMB, Sigma) HRP substrate was added to each well, and the absorbance of the yellow colour that developed after adding 0.5 M H₂SO₄ was measured at 450 nm.

The binding of IgG to human FcRn or human Fc γ receptors was examined as follows. His-tagged human FcRn was purified as previously described³¹, and His-tagged human Fc γ RIIIa, Fc γ RIIa and Fc γ RIIb were purchased from R&D Systems. Nickel-coated plates (96 well, Thermo Scientific) were coated with 2 $\mu\text{g ml}^{-1}$ His-tagged human FcRn or human Fc γ receptor and incubated at room temperature for 1 h. The ELISA was performed as described above. To examine the binding of monoclonal antibodies to human FcRn at pH 6.0, PBS at pH 6.0 was used instead of PBS at pH 7.4. EC₅₀ determination for human FcRn binding was calculated by computer-assisted nonlinear fitting using GraphPad Prism (Graphpad Software).

VRC01 and its mutants were quantified as follows. ELISA plates (96 well) were coated with 2 $\mu\text{g ml}^{-1}$ RSC3 in PBS, incubated at 4 °C overnight and blocked with PBS containing 5% BSA at room temperature for 1 h. Sera were diluted in 2.5% BSA in PBS and added to the plate and incubated at room temperature for 1 h, and the ELISA was carried out as described above. Purified monoclonal antibodies were used as a standard, and the limit of detection was 0.4 ng ml⁻¹.

Anti-VRC01 antibody responses were evaluated as follows. The sera from macaques that had been administered VRC01 or VRC01-LS were added to 96-well ELISA plates coated with $2 \mu\text{g ml}^{-1}$ VRC01 or VRC01-LS. To test VRC01-LS-specific antibody responses, the sera from the two groups were absorbed with $20 \mu\text{g ml}^{-1}$ VRC01, and the ELISA was carried out against VRC01-LS. The sera were diluted with TBS containing 5% skim milk, 2% BSA and 0.05% Tween 20, and the ELISA was performed as described above.

Neutralization assays

Antibody-mediated neutralization of pseudotyped HIV-1 isolates was measured using the TZM-bl luciferase reporter gene assay as described previously^{32–34}. The target baseline infection level was $\sim 200,000$ relative light units. Neutralization curves were fit using a five-parameter hill-slope equation as described previously³⁴. The concentrations of VRC01 and its mutants that were required to inhibit infection by 50% or 80% are reported as 50% or 80% inhibitory concentrations (IC_{50} or IC_{80}), respectively.

Biacore binding assays

For surface plasmon resonance analysis, human FcRn and human Fc γ RIIIa ($5 \mu\text{g ml}^{-1}$ in 10 mM acetate, pH 5.5, for 10 min at a $10 \mu\text{l min}^{-1}$ flow rate) were immobilized on a Biacore CM5 Sensor Chip to an immobilization level of ~ 500 response units (RU). VRC01 and its Fc mutants were injected for 2 min at various concentrations (0.01 – $10 \mu\text{M}$) and allowed to dissociate for 3 min at a $50 \mu\text{l min}^{-1}$ flow rate. The human FcRn surface was regenerated by two sequential injections of $1 \times$ PBS (pH 7.4) for 1 min at an $80 \mu\text{l min}^{-1}$ flow rate, while the human Fc γ RIIIa surface was regenerated with two sequential injections of 10 mM glycine (pH 2.1). All binding affinities were calculated using a 1:1 Langmuir fitting equation and Scrubber 2 (BioLogic Software), with an average value determined over the range of concentrations measured.

Animals

mFcRn^{-/-} hFcRn(276)^{Tg/Tg} mice were obtained from Jackson Laboratories (stock number 004919). They were housed and bred in the animal facility of the Vaccine Research Center (VRC) at the National Institute of Allergy and Infectious Diseases. *Macaca mulatta* animals of Indian origin and *Macaca fascicularis* were used in the non-human primate study. All animal experiments were reviewed and approved by the Animal Care and Use Committee of the VRC, and all animals were housed and cared for in accordance with local, state, federal and institutional policies in a facility accredited by the American Association for Accreditation of Laboratory Animal Care at the National Institutes of Health. Animal numbers per group in this study were chosen in accordance with previously published papers^{13,15,16}. Animals were chosen and randomized based on age and weight.

ADCC assay

ADCC assays were performed using a fluorescence activated cell sorting (FACS)-based method, as previously described²⁰. Briefly, HIV-IIIb-infected CEM NK^R-CCR5 cells were used as target cells and human peripheral blood mononuclear cells were used as effector cells. Target cells were double-stained with the fluorescent dyes PKH26 (Sigma) and

carboxyfluorescein succinimidyl ester (CFSE; Invitrogen). Target cells (10,000) and serially diluted monoclonal antibody were added to each well of a 96-well plate, mixed thoroughly and incubated at room temperature for 15 min. Effector cells (500,000) were added to each well and mixed thoroughly. The plate was centrifuged for 3 min at 400 r.p.m. and incubated at 37 °C in a 5% CO₂ incubator for 4 h. The cells were washed with PBS, fixed with 1% paraformaldehyde in PBS, and stored at 4 °C overnight. The percentage of CFSE⁺ cells within the PKH26^{hi} population was obtained by using an LSR-II flow cytometer (BD Biosciences) and FlowJo software (TreeStar). Non-stained and single-stained targets were included in every experiment to compensate for single-stained CFSE and PKH26 emissions.

Transcytosis assay

Assessments of transcytosis of VRC01 and its Fc mutants were performed as previously described for IgG³⁵. Briefly, MDCK cells were transfected to express human β_2 -microglobulin and human FcRn or vector controls and were grown to confluence in DMEM containing 10% FBS and 1% penicillin and streptomycin on 12-mm transwells with a pore size of 0.4 μm (Corning) and allowed to polarize for 96 h. Twelve hours before the commencement of transcytosis experiments, the medium was changed to serum-free medium without antibiotics. On the day of the experiment, the measured transepithelial resistance ranged between 150 and 200 Ωcm^2 . Transwells were incubated in Hank's balanced salt solution (HBSS), pH 7.4, for 20 min followed by equilibration at 36 °C and 5% CO₂ in a 12-well plate containing HBSS, pH 6.0, in the input chamber and HBSS, pH 7.4, in the output chamber. pH 6.0-adjusted VRC01 variants at varying concentrations in HBSS were then directly added to the input chamber. After incubating for 2 h at 36 °C and 5% CO₂, the medium in the output chamber was collected, and the monoclonal antibody concentrations were quantified by ELISA. Mycoplasma-free stocks of transfected MDCK cells using the Venor GeM Mycoplasma Detection Kit (Sigma, MP0025) were maintained as aliquots and regularly thawed for use every 3–4 weeks.

Pharmacokinetic experiments in rhesus macaques

Female Indian rhesus macaques weighing between 2.9 and 6.7 kg were randomly assigned to groups according to body weight (four macaques per group for VRC01 and VRC01-LS, and two macaques per group for VRC01-IHH) and were intravenously injected with 10 mg kg⁻¹ monoclonal antibody. Blood was collected before injection on day 0, at 30 min and 6 h after injection, and at 1, 2, 4, 7, 14, 21 and 28 days after injection. The concentration of each monoclonal antibody was quantified by ELISA. Pharmacokinetic parameters were calculated with a two-compartment model using the WinNonlin software (Pharsight).

Immunohistochemical staining

All staining procedures were performed as previously described³⁶, using 5- μm tissue sections mounted on glass slides. Tissues were deparaffinized and rehydrated in deionized water. Heat-induced epitope retrieval was performed using a water bath (98 °C) in EDTA Decloaker (Biocare Medical), followed by cooling to room temperature. Tissue sections were then blocked with Sniper blocking reagent (Biocare Medical) for 30 min at room temperature. RSC3-biotin was diluted at 1:100 in TNB (0.1 M Tris-HCl, pH 7.5, 0.1 M NaCl and 0.05% Tween 20 with DuPont Blocking Reagent) and incubated overnight at 4 °C.

After the RSC3–biotin incubation, the sections were washed with PBS containing 0.1% Tween 20 and then incubated with anti-biotin antibody conjugated to alkaline phosphatase in TNB for 2 h at room temperature. After the incubation with anti-biotin antibody, the sections were washed with PBS containing 0.1% Tween 20. Signal was detected with the Warp Red Chromogen Kit (Biocare Medical). The sections were counterstained with Harris Hematoxylin (Surgipath), dehydrated rapidly in a gradient of ethanols and mounted with Permount (Fisher Scientific). Stained sections were examined by light microscopy at ambient temperatures. Light micrographs were taken using an Olympus BX60 upright microscope with the following objectives: $\times 10$ (0.3 NA), $\times 20$ (0.5 NA) and $\times 40$ (0.75 NA); images were acquired using a SPOT colour mosaic camera (model 11.2; Diagnostic Instruments) and SPOT acquisition software (version 4.5.9; Diagnostic Instruments). Anti-biotin antibody conjugated to alkaline phosphatase was used as a negative control antibody in all instances and yielded negative staining results. For staining of human FcRn, heat-induced epitope retrieval was performed in Diva Decloaker (Biocare Medical) at 96 °C for 20 min, and polyclonal anti-human-FcRn antibody (1:50 dilution; Sigma, HPA012122) and anti-rabbit IgG conjugated to alkaline phosphatase were used as primary and secondary antibodies, respectively.

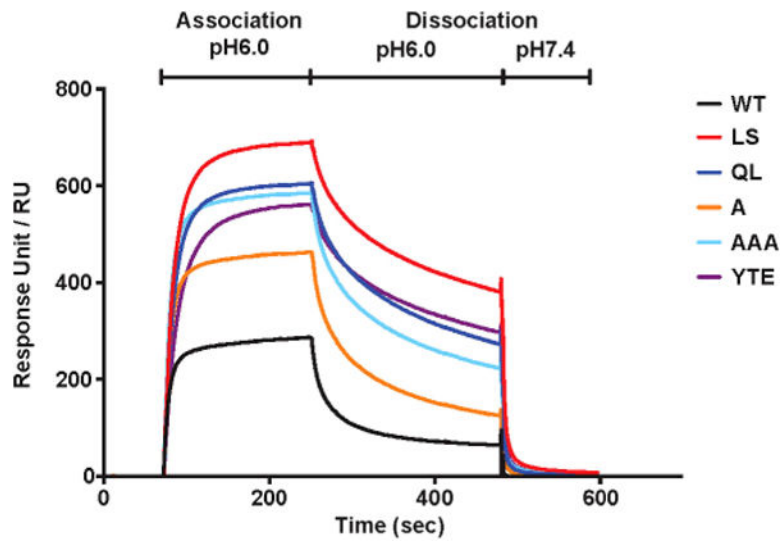
Quantitation of monoclonal antibodies in rectal biopsies

As previously described³⁷, rectal biopsy samples were added to 1.5-ml tubes containing 100 μ l PBS with EDTA-free protease inhibitor (Roche). The samples were ground on ice for 30 s and centrifuged at 4 °C for 20 min at 12,000 r.p.m., and the supernatants were collected. The total protein amounts were quantified by a BCA Protein Assay Kit (Thermo Scientific), and VRC01 and its Fc mutants were quantified by ELISA. The monoclonal antibody amount per mg of total protein is shown. The trends over days 2–28 were compared between groups by assuming a linear model for each animal and then testing the parameters from the linear models for differences between groups using a two-tailed *t*-test.

Challenge experiment in rhesus macaques

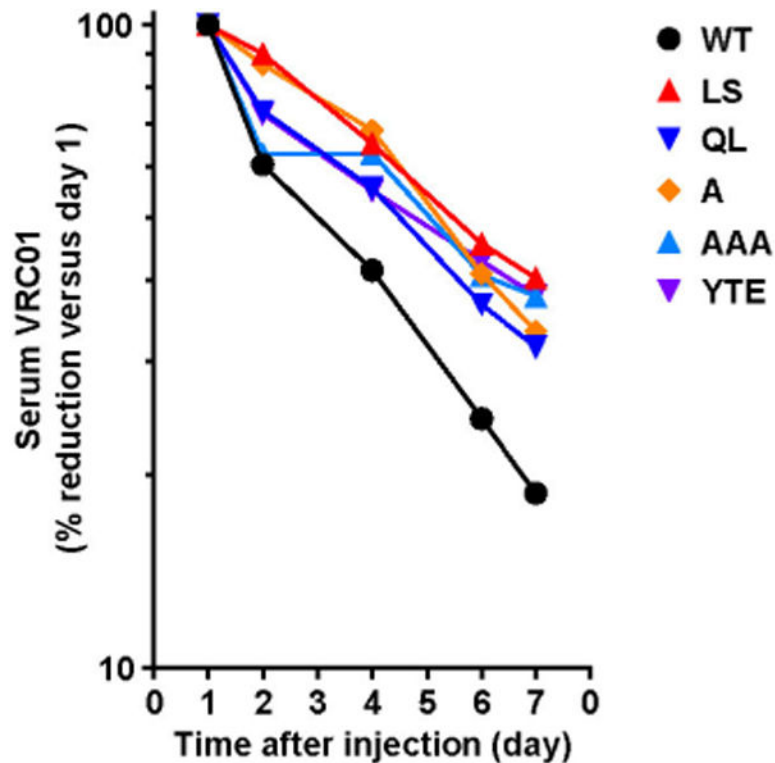
Male Indian rhesus macaques weighing 3.2–4.8 kg were randomly assigned to groups according to body weight, intravenously injected with 0.3 mg kg⁻¹ each monoclonal antibody and intrarectally challenged with undiluted SHIV BaLP45 days after the monoclonal antibody injection. Blood was collected twice a week for up to 4 weeks and then once a week for up to 12 weeks. Plasma was isolated from the blood samples. The plasma viral RNA levels were determined using a modified two-step quantitative reverse transcription PCR process. Experimental samples were run in parallel with a simian immunodeficiency virus (SIV) *gag* RNA standard on an Applied Biosystems StepOne Real-Time PCR System. The lower limit of detection using this assay was 250 copies of SIV RNA ml⁻¹. The forward primer used was 5'-GTC TGC GTC ATC TGG ATT C-3', and the reverse primer was 5'-CAC TAG GTG TCT CTG CAC TAT CTG TTT TG-3'.

Extended Data



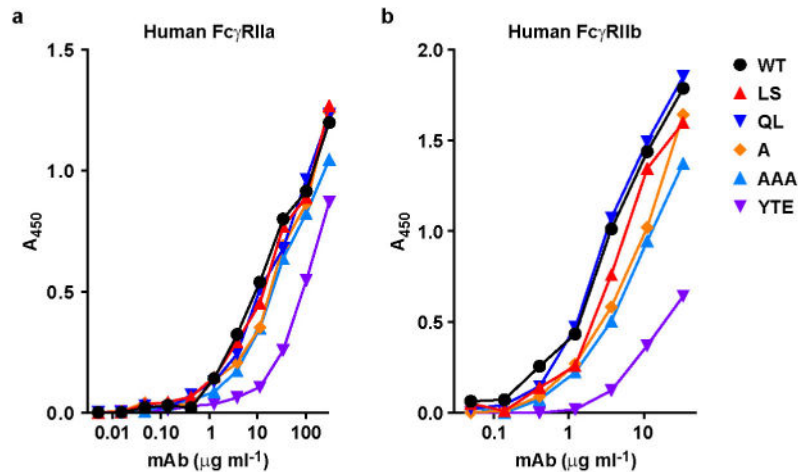
Extended Data Figure 1. Enhanced FcRn-binding mutants of VRC01 are released from human FcRn at pH 7.4

VRC01 or the indicated FcRn-binding mutants were injected in PBS (pH 6.0) at a concentration of 100 nM over human-FcRn-immobilized Biacore CM5 sensor chips (~500 response units (RU)) and were dissociated using PBS at pH 6.0 followed by PBS at pH 7.4.



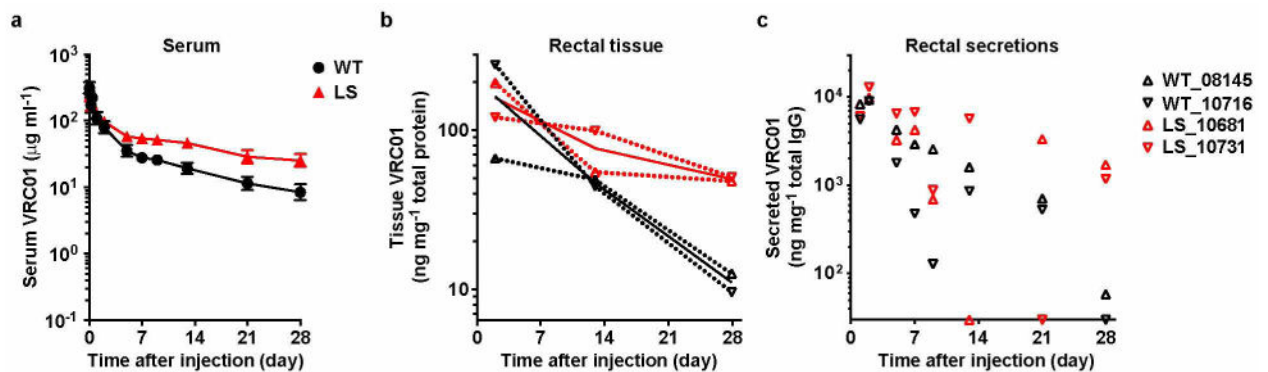
Extended Data Figure 2. Mutants with enhanced human FcRn binding persist at higher serum concentrations than VRC01 in the human-FcRn(276)-transgenic mouse

The indicated VRC01-derived monoclonal antibodies (2 mg kg^{-1}) were injected intravenously into 6–8-week-old human-FcRn(276)-transgenic mice ($n = 4$, male and female mice evenly distributed). Serum concentrations were assessed by indirect ELISA against RSC3 over time. The percentage of the monoclonal antibodies remaining in the serum is shown compared with the percentage on day 1 (set at 100%).



Extended Data Figure 3. Binding of VRC01, VRC01-LS and other FcRn-binding mutants to Fc γ RIIa and Fc γ RIIb

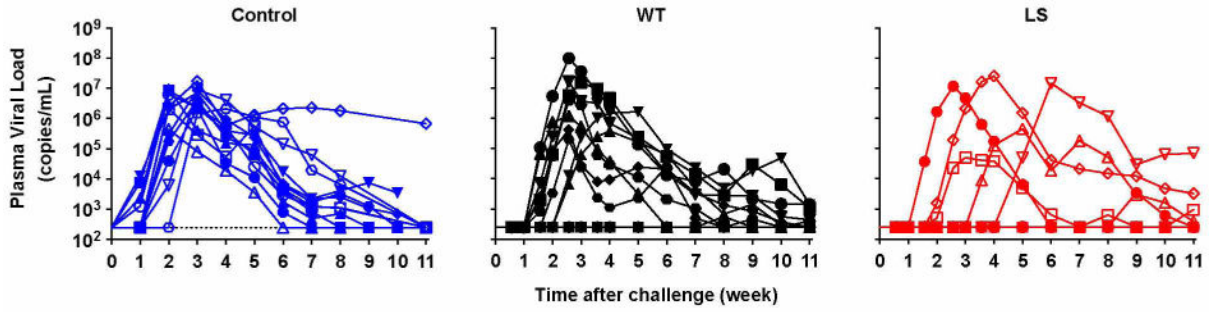
Binding to the indicated human Fc receptors was evaluated by ELISA as described in Methods.



Extended Data Figure 4. Serum pharmacokinetics, rectal tissue accumulation and mucosal secretion of VRC01-derived monoclonal antibodies in cynomolgus macaques

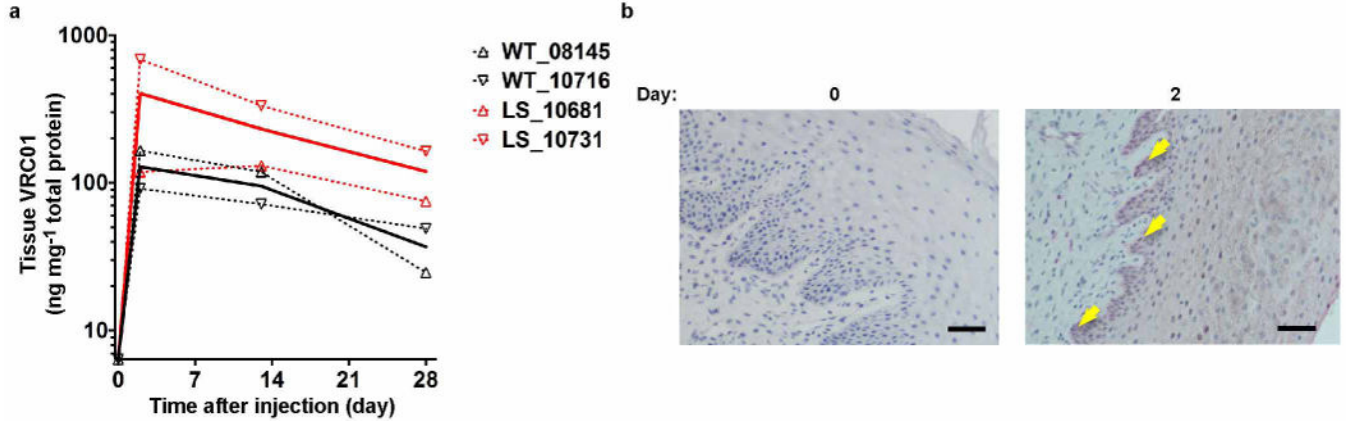
VRC01 or VRC01-LS (10 mg kg^{-1}) were injected intravenously into cynomolgus macaques.

a, The serum levels ($n = 4$) were analysed over time. **b**, **c**, The amounts of monoclonal antibody per mg of total tissue protein in rectal biopsy samples (**b**) and per mg of total IgG in rectal secretions (**c**) from each monoclonal-antibody-injected cynomolgus macaque ($n = 2$ per group) were quantitated and are shown over time. The values for each macaque and the mean values for the groups are shown as dotted lines and heavier solid lines, respectively (**b**). Pharmacokinetic parameters were calculated with a two-compartment model (VRC01 versus VRC01-LS, half-life, 9.0 versus 30.3 days; clearance, 15.7 versus $3.7 \text{ ml day}^{-1} \text{ kg}^{-1}$; area under the curve (AUC), 896 versus $2,812 \text{ day} \times \mu\text{g ml}^{-1}$).



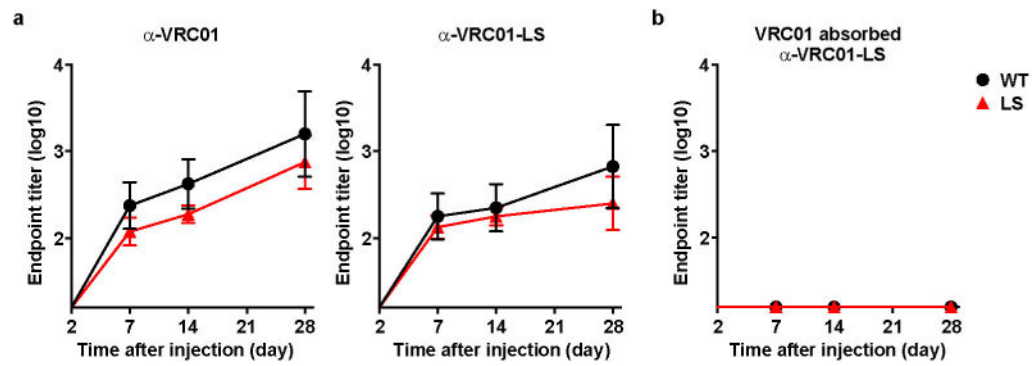
Extended Data Figure 5. Viral load measurements over time after passive antibody transfer and SHIV challenge of non-human primates

The indicated monoclonal antibodies (0.3 mg kg^{-1}) were administered intravenously to rhesus macaques ($n = 12$). Macaques were challenged with SHIV BaLP4 5 days later, and the plasma viral loads were measured over time. Normal human IgG was given to the control group. Five of 12 VRC01-LS-injected macaques and 10 of 12 VRC01-injected macaques were infected ($P = 0.0447$, one-tailed Fisher's exact test).



Extended Data Figure 6. Accumulation and localization of VRC01 in vaginal tissue

a, VRC01 or VRC01-LS (10 mg kg^{-1}) were injected intravenously into female cynomolgus macaques ($n = 2$). The monoclonal antibody concentration per mg of total tissue protein in vaginal biopsy samples was quantitated at the indicated times. The values for each macaque and the mean values for the groups are shown as dotted and solid lines, respectively. **b**, VRC01 (20 mg kg^{-1}) was injected intravenously into rhesus macaques ($n = 2$), and vaginal biopsy samples were taken and processed. Immunohistochemical staining was performed before and after the antibody dosing. The arrows indicate VRC01 (RSC3 staining, red) in basal and parabasal epithelial cells. The sections are representative of the sections assessed for two macaques. Scale bar, $50 \mu\text{m}$.



Extended Data Figure 7. Similar antibody responses to VRC01 and VRC01-LS in non-human primates

VRC01 or VRC01-LS (10 mg kg^{-1}) was injected intravenously into Indian rhesus macaques ($n = 4$). **a**, Anti-VRC01 antibody responses (left) or anti-VRC01-LS antibody responses (right) were evaluated by ELISA. **b**, Sera from animals that were administered VRC01 or VRC01-LS were absorbed with $20 \mu\text{g ml}^{-1}$ VRC01, and binding to VRC01-LS was then evaluated by ELISA.

Extended Data Table 1
Comparative potency of HIV-1 neutralization by VRC01 and enhanced FcRn-binding mutants

	IC ₅₀ (µg/mL)*					
	WT	LS	QL	A	AAA	YTE
Q23.17	0.063	0.082	0.067	0.074	0.080	0.079
Q842.d12	0.020	0.028	0.020	0.019	0.019	0.021
YU2	0.139	0.166	0.144	0.168	0.154	0.176
JR-FL	0.026	0.031	0.027	0.027	0.027	0.032
7165.18	>50	>50	>50	>50	>50	>50
Du156.12	0.090	0.097	0.085	0.098	0.110	0.093
ZM109.4	0.094	0.154	0.109	0.136	0.084	0.188
SVA.MLV	>50	>50	>50	>50	>50	>50
SIVmac251.30	>50	>50	>50	>50	>50	>50

	IC ₈₀ (µg/mL)*					
	WT	LS	QL	A	AAA	YTE
Q23.17	0.162	0.228	0.195	0.204	0.227	0.239
Q842.d12	0.078	0.099	0.082	0.079	0.076	0.089
YU2	0.341	0.439	0.387	0.482	0.409	0.478
JR-FL	0.081	0.099	0.092	0.093	0.093	0.105
7165.18	>50	>50	>50	>50	>50	>50
Du156.12	0.255	0.279	0.263	0.290	0.295	0.284
ZM109.4	0.414	0.548	0.466	0.538	0.429	0.612
SVA.MLV	>50	>50	>50	>50	>50	>50
SIVmac251.30	>50	>50	>50	>50	>50	>50

* Values are colour coded according to their potency: white (>50 µg ml⁻¹), orange (0.1–1.0 µg ml⁻¹), and red (<0.1 µg ml⁻¹).

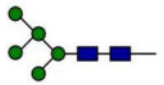
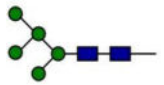
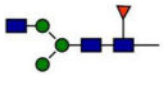
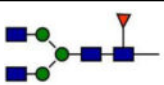
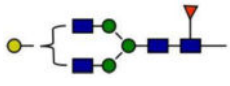
Extended Data Table 2

EC₅₀ values for the binding of VRC01 and VRC01-LS to human FcRn, as determined by ELISA

	EC ₅₀ (µg/mL)		Fold change
	pH6.0	pH7.4	pH7.4/pH6.0
WT	~20.00	>100.00	>5.00
LS	0.69	3.15	4.53
QL	0.87	4.60	5.27
A	1.35	6.69	4.97
AAA	0.95	4.61	4.82
YTE	0.83	4.01	4.86

Extended Data Table 3

Relative abundance of N297 glycosylation in VRC01 and VRC01-LS*

Glycan		Relative abundance (%)	
		WT	LS
Man ₅ GlcNAc ₂ (Man-5)		0.0	5.4
GlcNAc ₂ Man ₃ GlcNAcFuc		0.0	2.3
GlcNAc ₂ Man ₃ GlcNAc ₂ Fuc (GOF)		87.6	80.6
GalGlcNAc ₂ Man ₃ GlcNAc ₂ Fuc (G1F)		12.4	8.9

* Glycosylation was analysed by nanoLC-ESI-MS/MS (nano liquid chromatography electrospray ionization mass spectrometry) peptide sequencing technology.

Acknowledgments

We thank M. Roederer for advice on the design and statistical analysis of animal studies. This research was supported by the Intramural Research Program of the Vaccine Research Center, National Institute of Allergy and Infectious Diseases (NIAID), National Institutes of Health (NIH), and in part by a grant from the Foundation for the National Institutes of Health with support from the Collaboration for AIDS Vaccine Discovery (CAVD), award OPP1039775, from the Bill & Melinda Gates Foundation. R.S.B. is supported by the NIH (DK044319, DK051362, DK053056 and DK088199) and the Harvard Digestive Diseases Center (DK0034854). T.R. is supported by the German research foundation (DFG; RA 2040/1-1). The findings and conclusions in this report are those of the authors and do not necessarily reflect the views of the funding agencies.

References

1. Roopenian DC, Akilesh S. FcRn: the neonatal Fc receptor comes of age. *Nature Rev Immunol.* 2007; 7:715–725. [PubMed: 17703228]
2. Ward ES, Ober RJ. Multitasking by exploitation of intracellular transport functions: the many faces of FcRn. *Adv Immunol.* 2009; 103:77–115. [PubMed: 19755184]
3. Wu X, et al. Rational design of envelope identifies broadly neutralizing human monoclonal antibodies to HIV-1. *Science.* 2010; 329:856–861. [PubMed: 20616233]
4. Hessel AJ, et al. Fc receptor but not complement binding is important in antibody protection against HIV. *Nature.* 2007; 449:101–104. [PubMed: 17805298]
5. Nimmerjahn F, Ravetch JV. Fc γ receptors as regulators of immune responses. *Nature Rev Immunol.* 2008; 8:34–47. [PubMed: 18064051]
6. Hessel AJ, et al. Broadly neutralizing human anti-HIV antibody 2G12 is effective in protection against mucosal SHIV challenge even at low serum neutralizing titers. *PLoS Pathogens.* 2009; 5:e1000433. [PubMed: 19436712]
7. Walker LM, et al. Broad and potent neutralizing antibodies from an African donor reveal a new HIV-1 vaccine target. *Science.* 2009; 326:285–289. [PubMed: 19729618]
8. Hessel AJ, et al. Broadly neutralizing monoclonal antibodies 2F5 and 4E10 directed against the human immunodeficiency virus type 1 gp41 membrane-proximal external region protect against mucosal challenge by simian–human immunodeficiency virus SHIVBa-L. *J Virol.* 2010; 84:1302–1313. [PubMed: 19906907]
9. Walker LM, et al. Broad neutralization coverage of HIV by multiple highly potent antibodies. *Nature.* 2011; 477:466–470. [PubMed: 21849977]
10. Huang J, et al. Broad and potent neutralization of HIV-1 by a gp41-specific human antibody. *Nature.* 2012; 491:406–412. [PubMed: 23151583]
11. Moldt B, et al. Highly potent HIV-specific antibody neutralization *in vitro* translates into effective protection against mucosal SHIV challenge *in vivo*. *Proc Natl Acad Sci USA.* 2012; 109:18921–18925. [PubMed: 23100539]
12. Bitonti AJ, et al. Pulmonary delivery of an erythropoietin Fc fusion protein in nonhuman primates through an immunoglobulin transport pathway. *Proc Natl Acad Sci USA.* 2004; 101:9763–9768. [PubMed: 15210944]
13. Dall' Acqua WF, Kiener PA, Wu H. Properties of human IgG1s engineered for enhanced binding to the neonatal Fc receptor (FcRn). *J Biol Chem.* 2006; 281:23514–23524. [PubMed: 16793771]
14. Hinton PR, et al. An engineered human IgG1 antibody with longer serum half-life. *J Immunol.* 2006; 176:346–356. [PubMed: 16365427]
15. Petkova SB, et al. Enhanced half-life of genetically engineered human IgG1 antibodies in a humanized FcRn mouse model: potential application in humorally mediated autoimmune disease. *Int Immunol.* 2006; 18:1759–1769. [PubMed: 17077181]
16. Zalevsky J, et al. Enhanced antibody half-life improves *in vivo* activity. *Nature Biotechnol.* 2010; 28:157–159. [PubMed: 20081867]
17. Dall' Acqua WF, et al. Increasing the affinity of a human IgG1 for the neonatal Fc receptor: biological consequences. *J Immunol.* 2002; 169:5171–5180. [PubMed: 12391234]
18. Roopenian DC, et al. The MHC class I-like IgG receptor controls perinatal IgG transport, IgG homeostasis, and fate of IgG–Fc-coupled drugs. *J Immunol.* 2003; 170:3528–3533. [PubMed: 12646614]
19. Smalls-Mantey A, et al. Antibody-dependent cellular cytotoxicity against primary HIV-infected CD4⁺ T cells is directly associated with the magnitude of surface IgG binding. *J Virol.* 2012; 86:8672–8680. [PubMed: 22674985]
20. Gómez-Román VR, et al. A simplified method for the rapid fluorometric assessment of antibody-dependent cell-mediated cytotoxicity. *J Immunol Methods.* 2006; 308:53–67. [PubMed: 16343526]

21. Klein K, et al. Neutralizing IgG at the portal of infection mediates protection against vaginal simian/human immunodeficiency virus challenge. *J Virol*. 2013; 87:11604–11616. [PubMed: 23966410]
22. Kwong PD, Mascola JR, Nabel GJ. Broadly neutralizing antibodies and the search for an HIV-1 vaccine: the end of the beginning. *Nature Rev Immunol*. 2013; 13:693–701. [PubMed: 23969737]
23. Onorato IM, et al. Mucosal immunity induced by enhance-potency inactivated and oral polio vaccines. *J Infect Dis*. 1991; 163:1–6. [PubMed: 1845806]
24. Sicinski P, et al. Poliovirus type 1 enters the human host through intestinal M cells. *Gastroenterology*. 1990; 98:56–58. [PubMed: 2152776]
25. Yoshida M, et al. Human neonatal Fc receptor mediates transport of IgG into luminal secretions for delivery of antigens to mucosal dendritic cells. *Immunity*. 2004; 20:769–783. [PubMed: 15189741]
26. Keele BF, et al. Identification and characterization of transmitted and early founder virus envelopes in primary HIV-1 infection. *Proc Natl Acad Sci USA*. 2008; 105:7552–7557. [PubMed: 18490657]
27. Li Z, et al. Transfer of IgG in the female genital tract by MHC class I-related neonatal Fc receptor (FcRn) confers protective immunity to vaginal infection. *Proc Natl Acad Sci USA*. 2011; 108:4388–4393. [PubMed: 21368166]
28. Robbie GJ, et al. A novel investigational Fc-modified humanized monoclonal antibody, motavizumab-YTE, has an extended half-life in healthy adults. *Antimicrob Agents Chemother*. 2013; 57:6147–6153. [PubMed: 24080653]
29. Pegu A, et al. Neutralizing antibodies to HIV-1 envelope protect more effectively in vivo than those to the CD4 receptor. *Sci Transl Med*. 2014; 6:243ra88.
30. Edelman GM, et al. The covalent structure of an entire γ G immunoglobulin molecule. *Proc Natl Acad Sci USA*. 1969; 63:78–85. [PubMed: 5257969]
31. Gastinel LN, Simister NE, Bjorkman PJ. Expression and crystallization of a soluble and functional form of an Fc receptor related to class I histocompatibility molecules. *Proc Natl Acad Sci USA*. 1992; 89:638–642. [PubMed: 1530991]
32. Li M, et al. Human immunodeficiency virus type 1 *env* clones from acute and early subtype B infections for standardized assessments of vaccine-elicited neutralizing antibodies. *J Virol*. 2005; 79:10108–10125. [PubMed: 16051804]
33. Shu Y, et al. Efficient protein boosting after plasmid DNA or recombinant adenovirus immunization with HIV-1 vaccine constructs. *Vaccine*. 2007; 25:1398–1408. [PubMed: 17113201]
34. Seaman MS, et al. Tiered categorization of a diverse panel of HIV-1 Env pseudoviruses for assessment of neutralizing antibodies. *J Virol*. 2010; 84:1439–1452. [PubMed: 19939925]
35. Claypool SM, Dickinson BL, Yoshida M, Lencer WI, Blumberg RS. Functional reconstitution of human FcRn in Madin–Darby canine kidney cells requires co-expressed human β ₂-microglobulin. *J Biol Chem*. 2002; 277:28038–28050. [PubMed: 12023961]
36. Zeng M, et al. Cumulative mechanisms of lymphoid tissue fibrosis and T cell depletion in HIV-1 and SIV infections. *J Clin Invest*. 2011; 121:998–1008. [PubMed: 21393864]
37. Baker K, et al. Neonatal Fc receptor expression in dendritic cells mediates protective immunity against colorectal cancer. *Immunity*. 2013; 39:1095–1107. [PubMed: 24290911]

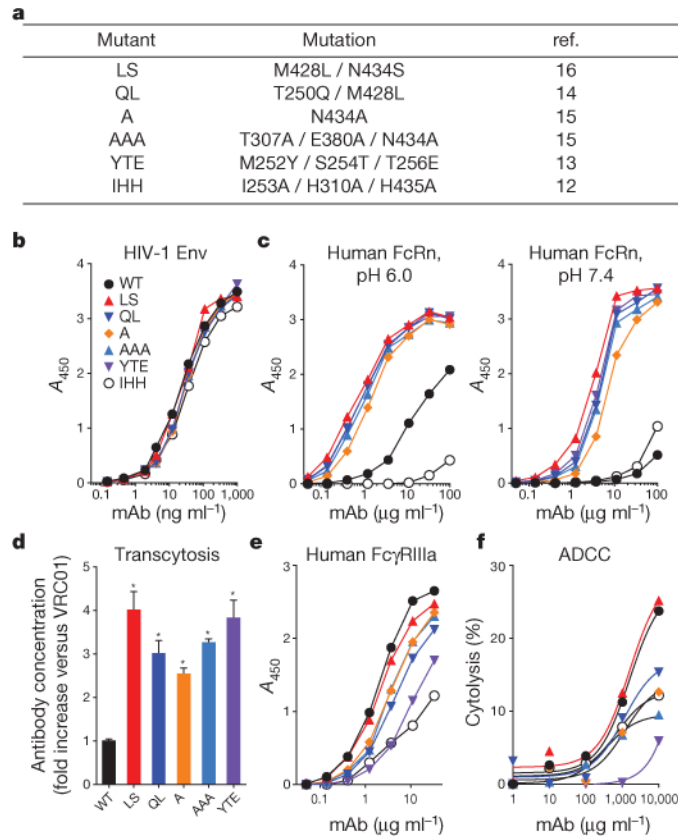


Figure 1. *In vitro* evaluation of VRC01 and its FcRn-binding mutants

a, The FcRn-binding mutations used in this study are shown. The IHH mutant does not bind to human FcRn, and the other mutations enhance binding to human FcRn. **b**, Binding to HIV-1 Env (RSC3, a resurfaced, stabilized core of HIV-1 gp120) was examined by ELISA. **c**, Binding to human FcRn was assessed at pH 6.0 and pH 7.4 by ELISA. **d**, Transcytosis was assessed by adding $1.0 \mu\text{g ml}^{-1}$ of each monoclonal antibody (mAb) to the basolateral side of a monolayer of MDCK cells that express human FcRn, which were grown on a transwell filter plate, and incubating for 2 h. The concentration of each antibody on the apical side was measured by quantitative RSC3 ELISA, and the fold increase in antibody concentration over VRC01 (WT) is shown. *, $P < 0.001$ versus VRC01, two-tailed Student's *t*-test. **e**, Binding to human FcγRIIIa was examined by ELISA. **f**, The ability of each monoclonal antibody to induce ADCC was analysed using human peripheral blood mononuclear cells as effector cells and HIV-1-infected CEM-NK^R cells as targets and staining with the fluorescent dyes PKH26 and carboxyfluorescein succinimidyl ester (CFSE). The percentage killing was calculated from the percentage of CFSE⁻ cells within the PKH26^{hi} population. Assays were performed in duplicate (**b**, **c**, **e**, **f**) or quadruplicate (**d**), and the data points represent the mean values (**b**, **c**, **e**, **f**) or the mean \pm s.e.m. (**d**). The data are representative of two independent experiments (**b**–**f**). A_{450} , absorbance at 450 nm.

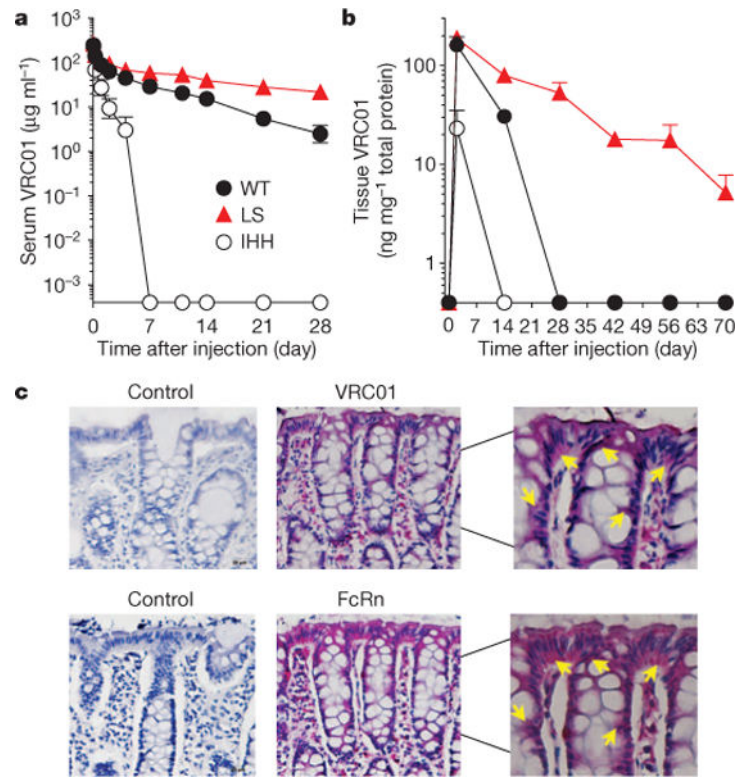


Figure 2. Pharmacokinetic study in Indian rhesus macaques

a, The indicated VRC01 variant monoclonal antibodies were injected intravenously at 10 mg per kg body weight into rhesus macaques on day 0 (VRC01 and VRC01-LS, $n = 4$; VRC01-IHH, $n = 2$), and the serum levels over time are shown. The pharmacokinetic parameters were calculated with a two-compartment model (VRC01 versus VRC01-LS, half-life, 4.7 versus 11.8 days; clearance, 16.5 versus 6.5 ml day⁻¹ kg⁻¹; area under the curve (AUC), 632 versus 1,645 day × µg ml⁻¹). **b**, The amount of monoclonal antibody per mg of total tissue protein in rectal biopsy samples from each monoclonal-antibody-injected rhesus macaque ($n = 4$ per group) was quantitated and is shown over time. VRC01-LS persisted at higher levels than did VRC01 ($P < 0.001$, two-tailed t -test). The data points are the mean ± s.e.m. **c**, Immunohistochemical staining of the rectal biopsy samples ($n = 6$ at 10 or 20 mg kg⁻¹ dose) after VRC01 administration shows co-localization of VRC01, as measured by indirect binding to an Env probe, RSC3 (VRC01, red; top) and FcRn, stained with an anti-human FcRn polyclonal antibody (FcRn, red; bottom). The sections shown are representative of those observed in the six macaques. The adjacent sections were stained with RSC3 and the anti-human FcRn polyclonal antibody in test samples. Buffer without RSC3 and control rabbit IgG were used as negative controls for VRC01 and FcRn staining, respectively. The arrows indicate VRC01 or FcRn staining in the cytoplasm of epithelial cells. The images were captured at ×20 original magnification, except for the right column, which shows magnified views of the centre column (×40 original magnification).

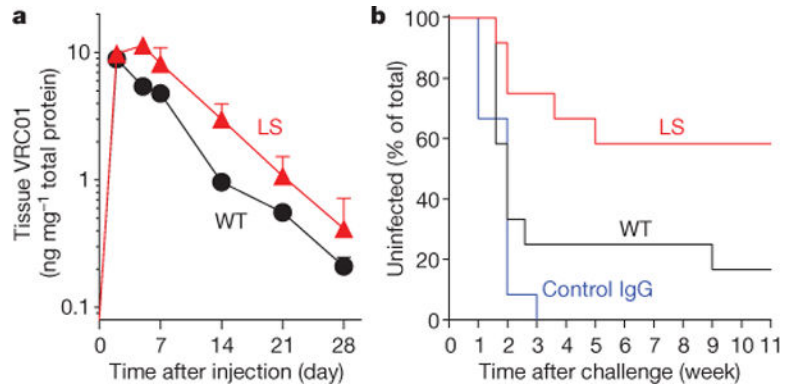


Figure 3. VRC01-LS affords greater protection against intrarectal SHIV BaLP4 challenge than VRC01

The indicated monoclonal antibodies were administered intravenously to rhesus macaques at a dose of 0.3 mg kg^{-1} on day 0. **a**, Monoclonal antibody levels per mg of total tissue protein in rectal biopsy samples ($n = 4$ per group) are shown over time. The data points are mean \pm s.e.m. **b**, The macaques ($n = 12$ per group) were challenged with SHIV BaLP4 on day 5 after monoclonal antibody administration, and the percentage of uninfected macaques was plotted over time. Normal human IgG was given to the control group. Five of 12 VRC01-LS-treated macaques and 10 of 12 VRC01-treated macaques were infected ($P = 0.0447$, one-tailed Fisher's exact test).

Table 1

Comparison of binding affinities for human FcRn and Fc γ RIIIa

Binding to bnAb		K_{on} (1/nM \times s)	K_{off} (1/s)	K_d (nM)	Fold K_d^*
Human FcRn (pH 6.0)	WT	0.000094	0.2790	3,000	1.00
	LS	0.000223	0.0558	250	12.00
	IHH	NB	NB	NB	-
Human Fc γ RIIIa	WT	0.000080	0.105	1,300	1.00
	LS	0.000099	0.100	1,010	1.29
	IHH	0.000041	0.187	4,500	0.29

* Fold change in K_d versus wild type (WT).

WT, VRC01; LS, VRC01-LS; IHH, VRC01-IHH (non-FcRn-binding mutant); K_{on} , association rate constant; K_{off} , dissociation rate constant; K_d , equilibrium dissociation constant; NB, not bound.